Journal of the Serbian Society for Computational Mechanics / Vol. 17 / No. 1, 2023 / pp 97-110
(10.24874/jsscm.2023.17.01.07)

NUMERICAL SIMULATION SHEAR-THICKENING FLUID THROUGH A SMALL-SCALED HEAT EXCHANGER

Hacène Hamoudi* **and Mohamed Bouzit**

[1] Department of Mechanical Engineering, University of Science and Technology of Oran, Mohammed Boudiaf, B.O. Box 1505, El-M'Naouer, 31000, Oran, Algeria
e-mail: hacenee22@hotmail.fr
**corresponding author*

Abstract

This paper aims to predict the behavior of a complex fluid though a small-sized thermal exchanger. The fluid used is of shear-thickening type of power-law index (n = 1.4) and Prandtl number (Pr = 50). The Ostwald model was utilized to define the dynamic viscosity. The exchanger consists of three rectangular cross-section tubes placed inside a thermally insulated chamber. The enclosure contains two ports for the entry and exit of the complex fluid. The complex fluid enters the chamber from the first port at a constant speed and at a low temperature, and then it passes around the hot tubes to be cooled. The rheological behavior of a fluid is defined by Ostwald equation, while the intensity of thermal buoyancy was modeled by Boussinesq approximation. The results showed that the increase of the velocity of the flow at the entrance increases the instability of the flow. Increasing the intensity of thermal buoyancy reduces the cooling process of the hot upper body.

Keywords: Heat transfer, mixed convection, shear-thickening fluid, micro-system.

1. Introduction

Heat exchanger is one of the necessary components in many technological and industrial applications. The purpose of the heat exchanger is to reduce the temperature of the hot elements and thus maintain integrity of the system. The most important fields of industry that have heat exchangers are: nuclear station, cooling systems in heat engines, heat treatment systems for pharmaceutical and food materials, cooling systems for electronic components.

The heat exchanger usually consists of two or more chambers. In the first chamber, a hot fluid passes through, and the heat is transmitted to the walls of the chamber. After that, another cold fluid passes around the hot chamber to cool it. This process allows the heated fluid to be cooled (Hajjar et al. 2022; Laidoudi and Ameur 2022a; Albadr et al. 2013; Laidoudi and Makinde 2021; Prabhanjan et al. 2002).

Recently, there have been a significant number of researches aimed at studying the heat transfer within thermal exchangers (Mokeddem et al. 2019; Alam and Kim 2018; Shirvan et al. 2016; Laidoudi and Bouzit 2017a; Nguyen and Ahn 2021). The papers can be classified into two main groups: the first group is concerned with studying the geometry of the heat exchanger

(Zimparov 2001; Laidoudi and Bouzit 2018; Kukulka et al. 2011; Fan et al. 2009; He et al. 2019), while the second aims to examine the effect of the fluid quality (Aliouane et al. 2021; Aissa et al. 2022a; Aissa et al. 2022b; Laidoudi et al. 2022; Laidoudi and Ameur 2022b). Previous work has been achieved either through real experimental (Peyghambarzadeh et al. 2011; Liu et al. 2006; Bouvier et al. 2003) or through numerical simulations (Laidoudi 2020a; Herouz et al. 2023; Mohammed et al. 2011). It was concluded that the numerical simulation can produce very accurate results in a short time with a profit.

With regard to previous papers that are relevant for the subject of our study, we should mention the following: Laidoudi and Ameur (2020) studied three classes of complex fluids using Ostwald model. The studied fluids were placed between two rotating cylinders, the inner one is hot and the outside one is cold. The aim of this research was to examine the ability of complex fluids to transfer thermal energy. Kefayati (2017) presented a work on the behavior of a non-Newtonian fluid of shear-thinning type inside a simple-shaped chamber. The fluid is characterized by a power-law index confined between 0.2 and 1. The research also includes the effect of thermal buoyancy effect referred to by the Richardson number, which is selected between 0.001 and 0.01. The results proved that the augmentation of the index (n) reduces the thermal activity of the fluid. Tizakast et al. (2021) conducted a comparative study between three types of fluids that have different values of power-law index (0.6, 1 and 1.4). The movement of the fluids was examined in a triangular chamber. The study showed that the forced convection has a high effectiveness on the rheological performance of the fluid.

Complex fluids are characterized by an irregular change in the viscosity. Sometimes, it increases in terms of the flow velocity and sometimes it decreases. The Ostwald mode is one of the most powerful models used in modeling the rheological aspect of the fluid. Many works have been achieved with this model (Laidoudi and Bouzit 2017b; Bouzit et al. 2018; Guendouci et al. 2021; Khezzar et al. 2012; Yaseen and Ismael 2020; Selimefendigil and Öztop 2016; Manchanda and Gangawane 2018). This model is distinguished by its ability to combine the Newtonian, shear-thickening and shear-thinning fluids.

Studies have shown that it is possible to improve the heat transfer inside the heat exchanger by searching for the geometry that reduces the friction between the flow and the geometry of the exchanger. Also, it was concluded that thermal activity of the exchanger can be strengthened by improving the thermal properties of the fluid, such as reducing the viscosity or increasing the heat capacity of the fluid. These conclusions have been drawn from many papers such as Laidoudi 2020b; Anouar and Mokhefi 2022; Helmaoui et al. 2020; Maneengam et al. 2022.

Through the aforementioned studies, it appears that there are still other ideas that have not been studied yet, especially those related to the combination of complex fluids and thermal buoyancy within small-sized heat exchangers. For this purpose, this paper is an initiative to support this idea. Accordingly, the work under examination is a numerical simulation of complex fluid of the shear-thickening fluid type inside a small-sized thermal exchanger. The studied parameters here: the flow velocity at the inlet of the exchanger, the intensity of the thermal buoyancy force and the rheological pattern of the fluid. It should be noted that the simulation was modeled only in two-dimensions and the mentioned studied parameters were treated with non-dimensional quantities. Accordingly, the Reynolds number expresses the value of the flow velocity at the entrance, while the Richardson number determines the intensity of thermal buoyancy produced.

2. Description of studied domain and mathematical modeling

The domain to be studied is well presented in Fig. 1. It is a small-sized heat exchanger used in micro-systems. The exchanger consists of a square-section chamber with three hot-walled tubes of rectangular cross-section. The exchanger has two equal-sized openings for the entry and exit of the flow. The exchanger dimensions are shown in Table 1. The outer walls of the exchanger are thermally insulated. The low-temperature complex fluid enters through the first port, passes around the hot bodies, and exits through the second port. The flow enters at a constant and definite velocity. The aim of this research is to examine the ability of the shear-thickening fluid to cool the three bodies under different conditions, namely the flow velocity at the entrance and the intensity of the thermal buoyancy force. The fluid has the power-law index value (n = 1.4) and thermal properties are given by Pr = 50 (of Prandlt number).

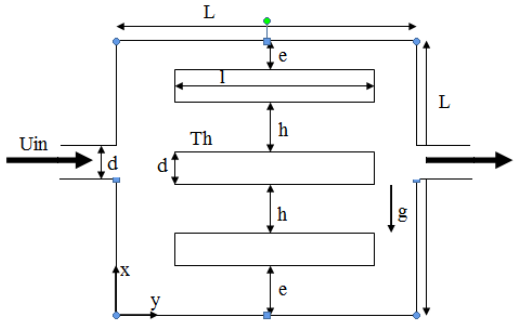

Fig. 1. Studied domain.

L	h/L	d/L	e/L	l/L
4 cm	0.75	0.125	0.1875	0.3125

Table 1. Dimensions of the studied geometry.

The numerical simulation of the study took place in two dimensions (2D), as the differential equations defined for physical phenomena are given in Cartesian coordinate system as follows (Kefayati, 2014):

$$\frac{\partial u}{\partial x}+\frac{\partial v}{\partial y}=0 \tag{1}$$

$$u\left(\frac{\partial u}{\partial x}\right)+v\left(\frac{\partial u}{\partial y}\right)=-\frac{1}{\rho}\frac{\partial p}{\partial x}+\frac{1}{\rho}\left(\frac{\partial \tau_{xx}}{\partial x}+\frac{\partial \tau_{xy}}{\partial y}\right) \tag{2}$$

$$u\left(\frac{\partial v}{\partial x}\right)+v\left(\frac{\partial v}{\partial y}\right)=-\frac{1}{\rho}\frac{\partial p}{\partial y}+\frac{1}{\rho}\left(\frac{\partial \tau_{xy}}{\partial x}+\frac{\partial \tau_{yy}}{\partial y}\right)+\beta g(T-T_c) \tag{3}$$

$$u\left(\frac{\partial T}{\partial x}\right)+v\left(\frac{\partial T}{\partial y}\right)=\alpha\left(\frac{\partial^2 T}{\partial x^2}+\frac{\partial^2 T}{\partial y^2}\right) \tag{4}$$

Ostwald model was adopted to define the dynamic viscosity of the shear-thickening fluid, the shear stress in eq. (2) and (3) are given as (Kefayati, 2014):

$$\tau_{ij} = m\left(2\left[\left(\frac{\partial u}{\partial x}\right)^2 + \left(\frac{\partial v}{\partial y}\right)^2\right] + \left(\frac{\partial u}{\partial x} + \frac{\partial v}{\partial y}\right)^2\right)^{(n-1)/2}\left(\frac{\partial u_i}{\partial x_j} + \frac{\partial u_j}{\partial x_i}\right) \tag{5}$$

where m is the consistency parameter and n is the power-law index. If n = 1, the fluid is Newtonian. If (n < 1), the fluid is shear-thinning. If (n > 1), the fluid is shear-thickening. The shear-thickening fluid means that the dynamic viscosity increases as the shear stress increases. That is, the dynamic viscosity can be written as:

$$\mu = m\left(\frac{I_2}{2}\right)^{\left(\frac{n-1}{2}\right)} \tag{6}$$

The dimensionless numbers of Reynolds, Prandtl and Richardson are given as:

$$Re = \frac{\rho(U_{in})^{2-n} d^n}{m}, Pr = \frac{mC_p}{k\left(\frac{U_{in}}{d}\right)^{n-1}}, Ri = \frac{Gr}{Re^2} = \frac{g\beta_T \Delta T d^3}{\left(U_{in}\right)^2} \tag{7}$$

According to the value of Richardson number, we distinguish three cases:

- Ri = 0, the heat transfer is pure forced convection;
- 0<Ri< 1, the heat transfer is mixed but the forced is the dominant;
- Ri = 1, the heat transfer is mixed, the natural and forced convections are equal.

The following expressions show how the dimensional quantities of length, velocity, pressure and temperature can be transformed to dimensionless:

$$(X,Y) = \frac{(x,y)}{d}, (U,V) = \frac{(u,v)}{U_{in}}, P = \frac{p}{\rho U_{in}^2}, T^* = \frac{(T - T_{in})}{T_w - T_{in}} \tag{8}$$

The dimensionless boundary conditions used the simulation:

- At the inlet port of the exchanger:

$$U = 1, V = 0, \theta = 0 \tag{9}$$

- At the outlet:

$$\frac{\partial U}{\partial X} = 0, \frac{\partial V}{\partial X} = 0, \frac{\partial \theta}{\partial X} = 0 \tag{10}$$

- On the heated bodies:

$$U = 0, V = 0, T^* = 1 \tag{11}$$

- On the chamber of the exchanger:

$$U = 0, V = 0, \frac{\partial T^*}{\partial n} = 0 \tag{12}$$

No-slip condition is selected on the walls of the bodies and cavity.

The mean Nusselt number of the heated body is calculated as:

$$Nu_L = \left(\frac{\partial T^*}{\partial n} \right)_{wall} \quad \text{and} \quad Nu = \frac{1}{A} \int_s Nu_L dA \tag{13}$$

The drag coefficient is obtained as:

$$C_D = \frac{F_D}{0,5 \rho U_{in}^2 d} \tag{14}$$

where F_D is the drag force exerted by the flow on the body.

3. Numerical methodology

The simulations are created using ANSYS-CFX numerical simulator. The latter transforms the differential equations into a system of matrices. And using the boundary conditions, solutions are calculated using the finite volume method. The results take into account that the error factor is less than the value 10^{-9} for continuity and momentum equations and 10^{-6} for energy equation. Furthermore, SIMPLEC algorithm used for pressure-velocity coupling and the convective terms was calculated according to high resolution schema.

At this stage, we make sure of the number of grid elements and their impacts on the calculation results. Four grids were produced with increasing density in the number of grid elements, after which the value of Nusselt number of the down, middle and upper bodies was calculated. The results of these calculations and the number of grid elements are shown in Table 2. By Table 2it is possible to deduce that there is stability in the values of Nusselt number for the three cylinders when the grid elements exceed the value 753,550. Therefore, this number is sufficient to calculate accurate values. The numerical stability can be deduced when the values of Nu become almost constant despite the increase in grid elements as in the case of G3 and G4.

Gird	Elements	Nu (C1)	Nu (C2)	Nu (C3)
G1	198,328	4.6670	4.9124	2.4344
G2	376,775	4.4523	4.6857	1.9889
G3	753,550	4.2213	4.5334	1.5431
G4	1507,100	4.2112	4.53102	1.5564

Table 2. Variation of Nu versus grid elements for n = 1, Re = 20 and Ri = 1.

This section is dedicated to demonstrating the effectiveness of the numerical method used in our paper. So, we recreated the work of Chatterjee and Amiroudine, (2010), which is a fluid flow around heated obstacles in a canal. The comparison results are shown in Fig. 2 where the results express the developments of the Nusselt number for the two obstacles in terms of the Reynolds number. We note here that there is a strong agreement in the results (between present data and the previous), and, therefore, we can say that our method is very effective in solving the differential equations of fluid mechanics and heat transfer.

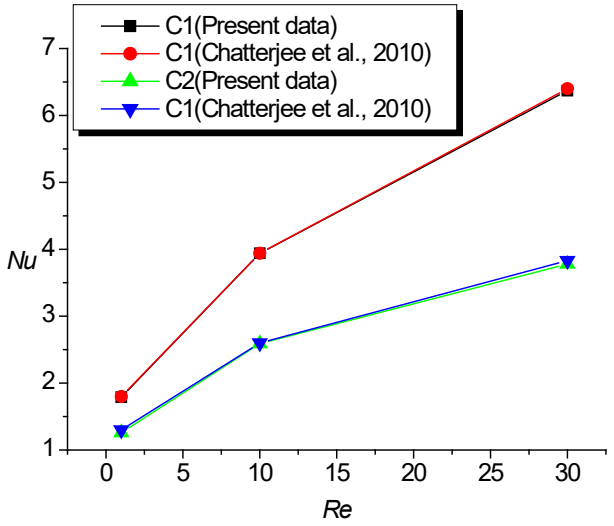

Fig. 2. Comparing the values of Nu of (Chatterjee and Amiroudine, 2010) in terms of Re for n = 1 and Ri = 1.

4. Results and discussion

The purpose of this paper is to present an investigation of the behavior of a complex fluid of the shear-thickening type inside a small-sized heat exchanger in order to know the process of cooling the hot parts. The qualitative criteria studied in this paper: the velocity of the flow at the entrance of the exchanger and the intensity of the thermal buoyancy force. Before starting to process the simulation results, it is worth recalling some basic concepts that contribute to the understanding of new results.

First, the fluid under study has a rheological property, which is that when the shear stress is high in a specific zone, the dynamic viscosity is also high. Secondly, the phenomenon of thermal buoyancy occurs when the layers of the fluid absorb a sufficient amount of heat, which makes them more expanding, and this is what makes them self-transfer upwards against the force of gravity. On the other hand, the cold layers become heavier, and therefore they are attracted towards the general gravitational force. Finally, the Reynolds number expresses the dynamic behavior of the fluid, and the increase in the value of this number as an indication of the augment of velocity of the flow at the entrance of the exchanger, whereas the Richardson number indicates the intensity of the thermal buoyancy, i.e. increasing the value of this number indicates that the difference in temperature between the hot and cold component increases.

Fig. 3 shows the streamlines in terms of the gradual increase in the Reynolds and Richardson numbers. Note that in the first case, for Ri = 0, the flow is symmetrical with respect to the line x= 0. And with increase in the value of Re, the flow spread increases, and small vortices appear at the entrance of the exchanger. On the other hand, the flow appears to lose symmetry by gradually increasing the value of the Richardson number because the hot fluid layers deviate upwards and the cold layers deviates downwards. This behavior causes the flow to deviate towards the bottom of the exchanger cavity. In addition to this, the downwards deflection of the flow creates steady vortices on the upper side of the system as shown in Fig. 3. It also appears that the higher the

value of the two numbers Re and Ri, results in the higherinstability of the flow. Furthermore, for Re = 5 there is almost no instability. For Re = 10, the instability starts for Ri = 1. For Re = 20, 30 and 40, the instability begins for Ri = 0.5.

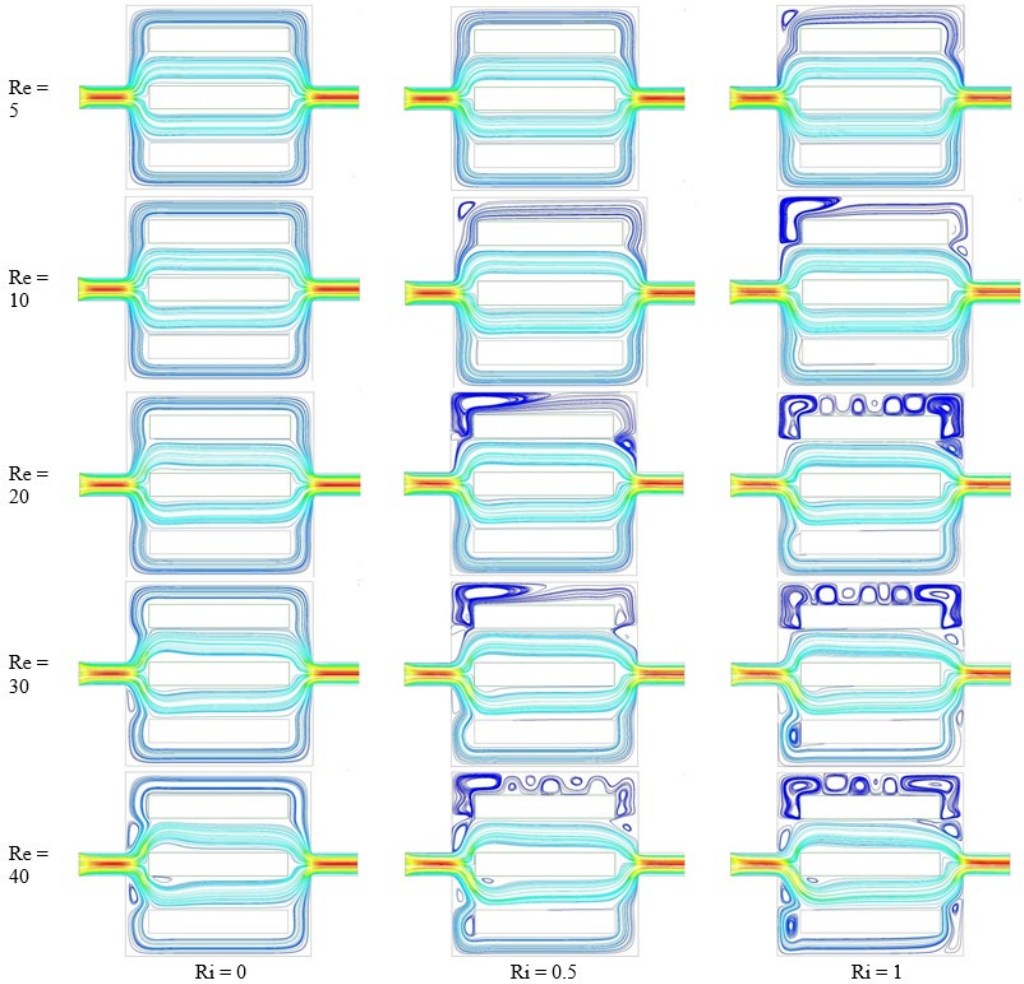

Fig. 3. Streamlines in the exchanger for different values of Re and Ri.

Fig. 4 shows the isotherms (dimensionless temperature) inside the exchanger in terms of the studied values of the two numbers Re and Ri. It is noted that the dimensionless temperature distribution is completely similar to motion diagrams (streamlines). Blue color indicates low dimensionless temperature (Tc) and it is for the flow entering the exchanger. We notice that when Ri = 0, the distribution of dimensionless temperatures is symmetrical with respect to (x = 0). The higher the value of Re, the greater the progression of low temperature into the room. on the other hand, with the presence of thermal buoyancy (Ri ≠ 0), we notice that the distribution of the low temperature is in the lower side of the container, while the upper side witnesses rise in temperature, which indicates the presence of flow stagnation in that side. Furthermore, when Ri = 0, the thermal transfer here is due to the velocity of the flow with which it entered the cavity, and this type is called forced convection whereas with the presence of thermal buoyancy, it is

called mixed convection. In general, this behavior of the fluid agrees well with what was previously observed by Chatterjee and Amiroudine 2010; and Laidoudi and Makinde 2021.

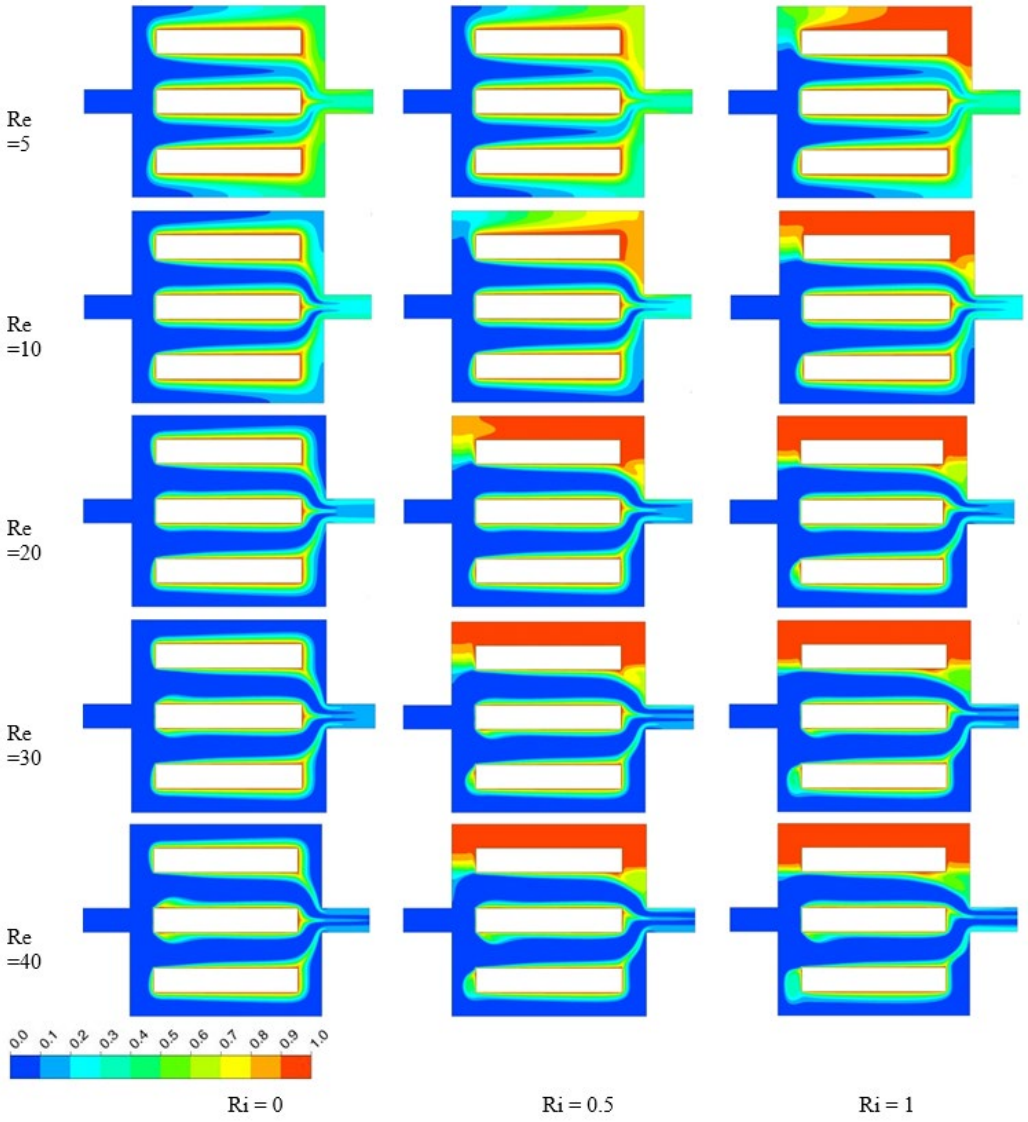

Fig. 4. Streamlines in the exchanger for different values of Re and Ri.

Fig. 5 shows the evolution of the mean values of Nusselt number (Nu) for the three hot bodies in terms of the Richardson and Reynolds numbers. Fig. 5 (a) for Ri = 0, Fig. 5 (b) for Ri = 0.5 and Fig. 5 (c) for Ri = 1. A high value of Nusselt number indicates an increase in thermal transfer of the hot body. Note that for all values of Ri (0, 0.5, and 1), increasing the value of Reynolds number augments the values of Nu for all bodies. In addition, when Ri = 0, the upper (C3) and low (C1) bodies have equal values of Nusselt number. On the other hand, the body in the middle (C2) has the maximum values of Nusselt number. With the effect of thermal buoyancy and its intensity increasing, the values of the Nusselt number for the body in the middle (C2) remains

the highest. In contrast, for the lower body (C1), the values of the Nusselt number rise as the Richardson number increases. For the upper body, the higher the value of Ri, the lower the Nusselt number.

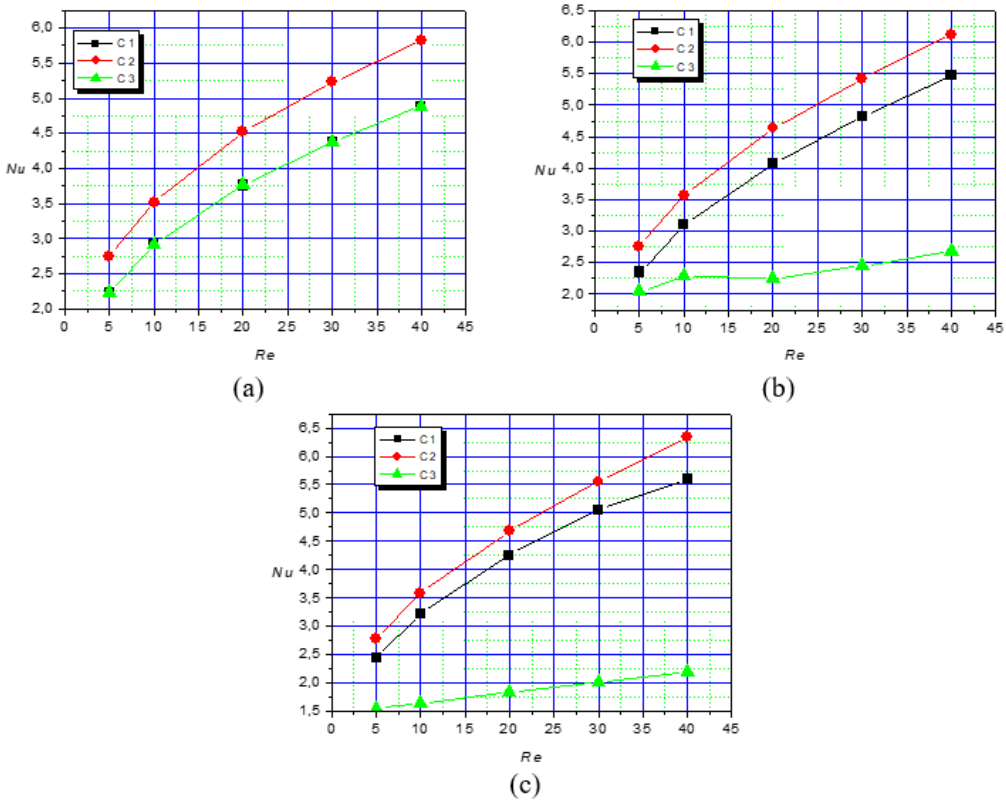

Fig. 5. Variations of Nu in terms of Re and for three bodies. (a) for Ri = 0. (b) for Ri = 0.5. (c) for Ri = 1.

Fig. 6 represents the evolutions of the drag coefficient of the three bodies (C1, C2 and C3) in terms of Richardson and Reynolds numbers. Fig. 6 (a) for Ri = 0, Fig. 6 (b) for Ri = 0.5 and Fig. 6 (c) for Ri = 1. This coefficient indicates the drag force that the flow applies to the objects. This force combines the pressure and frictional forces. We notice that the body in the middle (C2) is subjected to a higher drag force than the other bodies (C1 and C3) for all values of Re and Ri. In addition to this, we note that as the value of Ri increases, the drag coefficient of the upper body (C3) decreases, while the drag coefficient of the lower body (C1) increases. This can be explained by the fact that the flow entering the exchanger is cooler and this causes it to deflect downwards towards the lower body (C1). Therefore, the drag force increases on the lower body (C1) and decreases on the upper body (C3).

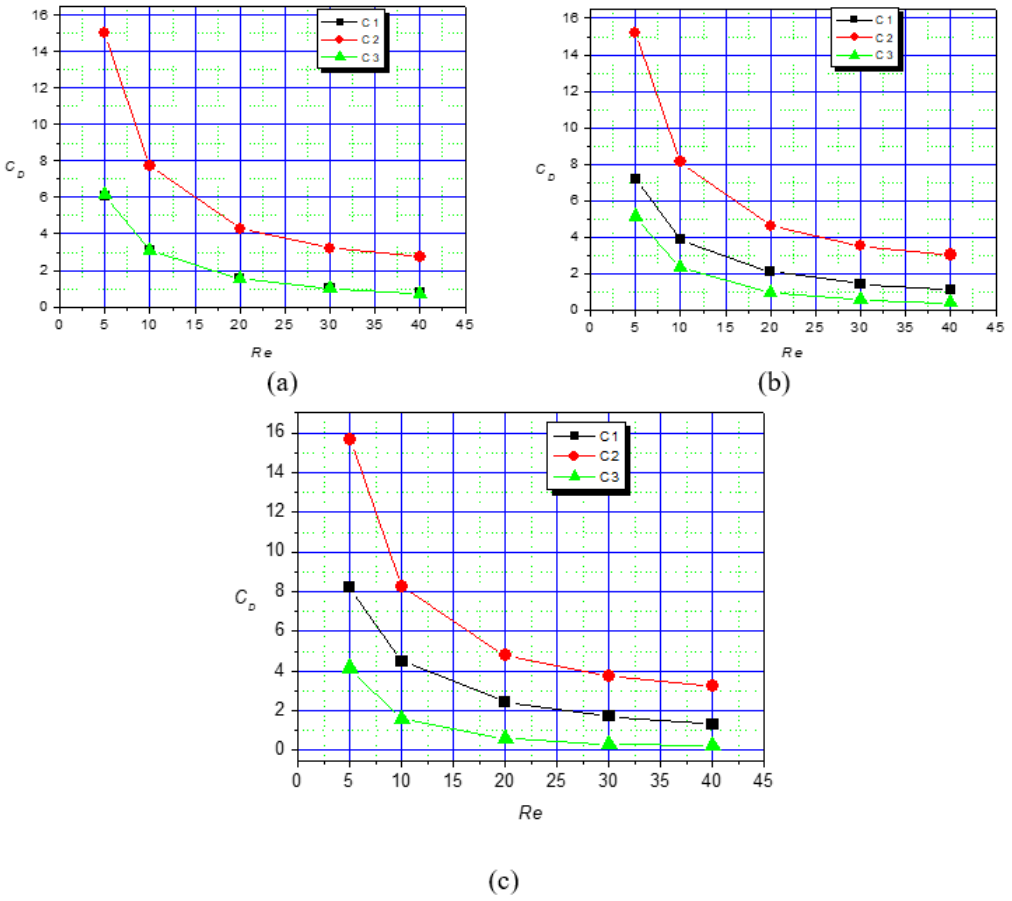

Fig. 6. Variations of C_D in terms of Re and for three bodies. (a) for Ri = 0. (b) for Ri = 0.5. (c) for Ri = 1.

5. Conclusion

Through this work, we seek to achieve a numerical simulation of a small-sized heat exchanger used in micro-systems. The fluid used is of the complex type of shear-thickening kind. The studied parameters are the velocity of the flow at the entrance of the exchanger, as well as the intensity of the thermal buoyancy. The study was achieved for these ranges: Re = 1 to 40, Ri = 0 to 1 at n = 1.4 and Pr = 50. At the end of the simulation, we reached the following concluding points:

- The increase in the value of Reynolds number increases the velocity of the flow at the entrance of the exchanger; the increase in the velocity of flow increasing the process of cooling the hot bodies and accordingly raises the values of Nusselt number.
- Gradual raise in the Richardson number increases the effect of thermal buoyancy. The higher this factor, the higher the heat transfer of lower body, which is in the middle, while it decreases the heat transfer of the upper body.

- The presence of thermal buoyancy causes a stagnation of fluid in the upper side of the chamber and causes the flow to deviate towards the bottom.
- With the presence of thermal buoyancy, the instability of the flow increases, especially with the increase in the velocity of the flow at the entrance of the exchanger.
- The object (C2) in the middle is subjected to a higher drag force than the other two objects.
- The higher the value of Ri, the more difficult it is to cool the upper body.
- For all values of Ri, a gradual increase in the Reynolds number decreases the drag coefficient of all bodies.

Nomenclature

d	diameter of obstacle [m]	u	velocity along x direction [m/s]
D	diameter of enclosure [m]	v	velocity along y direction [m/s]
g	gravity acceleration [ms^{-2}]	x	x-coordinate [m]
l	Width of orifices [m]	y	y-coordinate [m]
Nu_l	Average value of Nusselt number [-]	***Greek symbols***	
Nu	Local value of Nusselt number [-]	α	thermal diffusivity [m^2/s]
p	pressure [-]	β	coefficient of volume expansion [K^{-1}]
Pr	Prandtl number [-]	ν	kinematic viscosity [m^2/s]
Re	Reynolds number, [-]	ρ	density of fluid [kg/m^3]
Ri	Richardson number, [-]		
T_{in}	Temperature of flow [K]		
T_h	Temperature of obstacle [K]		

References

Aissa A, Al-Khaleel M, Mourad A, Laidoudi H, Driss Z, Younis O, Guedri K, Marzouki R (2022b). Natural convection within inversed T-shaped enclosure filled by nano-enhanced phase change material: Numerical investigation. Nanomaterials, 12, 2917.

Aissa A, Younis O, Al-Khaleel M, Laidoudi H, Akkurt N, Guedri K, Marzouki R, (2022a). 2D MHD mixed convection in a zigzag trapezoidal thermal energy storage system using NEPCM. Nanomaterials, 12, 3270.

Alam T, Kim M H, (2018). A comprehensive review on single phase heat transfer enhancement techniques in heat exchanger applications. Renewable and Sustainable Energy Reviews, 81, 813-839.

Albadr J, Tayal S, Alasadi M, (2013). Heat transfer through heat exchanger using Al2O3 nanofluid at different concentrations, Case Studies in Thermal Engineering, 1, 38-44.

Aliouane I, Kaid N, Ameur H, Laidoudi H, (2021). Investigation of the flow and thermal fields in square enclosures: Rayleigh-Bénard's instabilities of nanofluids, Thermal Science and Engineering Progress, 25, 100959.

Anouar Y, Mokhefi A, (2022). Numerical investigation of the nanofluid natural convection flow in a cpu heat sink using buongiorno tow-phase model. Journal of the Serbian Society for Computational Mechanics, 16, 13-42.

Bouvier P, Stouffs P, Bardon J P, (2005). Experimental study of heat transfer in oscillating flow. International Journal of Heat and Mass Transfer, 48, 2473-2482.

Bouzit F, Laidoudi H, Bouzit M, (2018). Simulation of power-law fluids and mixed convection heat transfer inside of curved duct. Defect and Diffusion Forum, 378, 113-124.

Chatterjee D, Amiroudine S (2010). Two-dimensional mixed convection heat transfer from confined tandem square cylinders in cross-flow at low Reynolds numbers. Communications in Heat and Mass Transfer, 37, 7–16.

Fan J F, Ding W K, Zhang JF, He Y L, Tao W Q (2009). A performance evaluation plot of enhanced heat transfer techniques oriented for energy-saving. International Journal of Heat and Mass Transfer, 52, 33-44.

Guendouci I, Laidoudi H, Bouzit M (2021). The effect of fin length on free convection heat transfer in annular space of concentric arrangement using shear-thinning fluids as a thermal medium, Defect and Diffusion Forum, 409, 194-204.

Hajjar A, Mehryan SAM, Ghalambaz M, (2020). Time periodic natural convection heat transfer in a nano-encapsulated phase-change suspension. International Journal of Mechanical Sciences, 166, 105243.

Helmaoui M, Laidoudi H, Belbachir A, Ayad A, Ghaniam A, (2020). Forced convection heat transfer from a pair of circular cylinders confined in ventilated enclosure. Diffusion Foundations, 26, 104-111.

Herouz K, Laidoudi H, Aissa A, Mourad A, Guedri K, Oreijah M, Younis O (2023). Analysis of nano-encapsulated phase change material confined in a double lid-driven hexagonal porous chamber with an obstacle under magnetic field, Journal of Energy Storage, 61, 106736.

He Y L, Tang S Z, Tao W Q, Li M J, Wang F L (2019). A general and rapid method for performance evaluation of enhanced heat transfer techniques. International Journal of Heat and Mass Transfer, 145, 118780.

Kefayati G, (2014). FDLBM simulation of magnetic field effect on non-newtonian blood flow in a cavity driven by the motion of two facing lids. Powder Technology, 253, 325–337.

Kefayati G H R (2017). Mixed convection of non-Newtonian nanofluid in an enclosure using Buongiorno's mathematical model. International Journal of Heat and Mass Transfer, 108, 1481-1500.

Khezzar L, Siginer D, Vinogradov I, (2012). Natural convection of power law fluids in inclined cavities. International Journal of Thermal Sciences, 53, 8-17.

Kukulka D J, Smith R, Fuller K G, (2011). Development and evaluation of enhanced heat transfer tubes. Applied Thermal Engineering, 31, 2141-2145.

Laidoudi H, (2020a).Natural convection from four circular cylinders in across arrangement within horizontal annular space. Acta Mechanica et Automatica, 14, 98-102.

Laidoudi H, (2020b). Upward flow and heat transfer around two heated circular cylinders in square duct under aiding thermal buoyancy. Journal of the Serbian Society for Computational Mechanics, 14, 113-123.

Laidoudi H, Aissa A, Saeed A M, Guedri K, Weera W, Younis O, Mourad A and Marzouki R (2022). Irreversibility interpretation and MHD mixed convection of hybrid nanofluids in a 3D heated lid-driven chamber. Nanomaterials, 12, 1747.

Laidoudi H and Ameur H (2020). Investigation of the mixed convection of power-law fluids between two horizontal concentric cylinders: Effect of various operating conditions, Thermal Science and Engineering Progress, 20, 100731.

Laidoudi H and Ameur H (2022a). Natural convection between hot and cold cylinders in enclosed space filled with copper-water nanofluid. Journal of Thermal Engineering, 8, 606-618.

Laidoudi H and Ameur H (2022b). Complex fluid flow in annular space under the effects of mixed convection and rotating wall of the outer enclosure, Heat Transfer, 51, 3741-3767.

Laidoudi H and Bouzit M, (2017a). The effect of asymmetrically confined circular cylinder and opposing buoyancy on fluid flow and heat transfer. Defect and Diffusion Forum, 374, 18-28.

Laidoudi H and Bouzit M (2017b). Mixed convection heat transfer from confined tandem circular cylinders in cross-flow at low Reynolds number, Mechanics, 23, 522-527.

Laidoudi H and Bouzit M (2018). The effects of aiding and opposing thermal buoyancy on downward flow around a confined circular cylinder, Periodica Polytechnica Mechanical Engineering, 62, 42-50.

Laidoudi H and Makinde OD (2021). Computational study of thermal buoyancy from two confined cylinders within a square enclosure with single inlet and outlet ports, Heat Transfer, 2021, 50, 1335-1350.

Liu Z, Wang Z and Ma C (2006). An experimental study on heat transfer characteristics of heat pipe heat exchanger with latent heat storage. Part I: Charging only and discharging only modes. Energy Conversion and Management, 47, 944-966.

Manchanda M and Gangawane K M, (2018). Mixed convection in a two-sided lid-driven cavity containing heated triangular block for non-Newtonian power-law fluids. International Journal of Mechanical Sciences, 144, 235-248.

Maneengam A, Laidoudi H, Abderrahmane A, Rasool G, Guedri K, Weera W, Obai Y and Bouallegue B (2022). Entropy generation in 2D lid-driven porous container with the presence of obstacles of different shapes and under the influences of Buoyancy and Lorentz forces. Nanomaterials, 12, 2206.

Mohammed H A, Gunnasegaran P and Shuaib N H (2011). Numerical simulation of heat transfer enhancement in wavy microchannel heat sink. International Communications in Heat and Mass Transfer, 38, 63-68.

Mokeddem M, Laidoudi H, Makinde OD andBouzit M (2019). 3D Simulation of incompressible poiseuille flow through 180 curved duct of square cross-section under effect of thermal buoyancy, Periodica Polytechnica Mechanical Engineering, 63, 257–269.

Nguyen D H and Ahn H S (2021). A comprehensive review on micro/nanoscale surface modification techniques for heat transfer enhancement in heat exchanger. International Journal of Heat and Mass Transfer. 178, 121601.

Peyghambarzadeh S M, Hashemabadi S H, Hoseini S M and Jamnani MS, (2011). Experimental study of heat transfer enhancement using water/ethylene glycol based nanofluids as a new coolant for car radiators. International Communications in Heat and Mass Transfer, 38, 1283-1290.

Prabhanjan D G, Raghavan G S V and Rennie T J, (2002). Comparison of heat transfer rates between a straight tube heat exchanger and a helically coiled heat exchanger. International Communications in Heat and Mass Transfer, 29, 185-191.

Selimefendigil F, Öztop H F (2016). MHD mixed convection and entropy generation of power law fluids in a cavity with a partial heater under the effect of a rotating cylinder, International Journal of Heat and Mass Transfer, 98, 40-51.

Shirvan K M, Ellahi R, Mirzakhanlari S, Mamourian M (2016). Enhancement of heat transfer and heat exchanger effectiveness in a double pipe heat exchanger filled with porous media: Numerical simulation and sensitivity analysis of turbulent fluid flow. Applied Thermal Engineering, 109, 761-774.

Tizakast Y, Kaddiri M, Lamsaadi M (2021). Double-diffusive mixed convection in rectangular cavities filled with non-Newtonian fluids. International Journal of Mechanical Sciences, 208, 106667.

Yaseen D T and Ismael M A (2020). Analysis of power law fluid-structure interaction in an open trapezoidal cavity. International Journal of Mechanical Sciences, 174, 105481.

Zimparov V (2001). Extended performance evaluation criteria for enhanced heat transfer surfaces: heat transfer through ducts with constant heat flux. International Journal of Heat and Mass Transfer, 44, 169-180.